Enhanced Seebeck coefficient through magnetic fluctuations in $Sr_2Ru_{1-x}M_xO_4$ (M = Co, Mn)

Takayoshi Yamanaka,* Ryuji Okazaki,† and Hiroshi Yaguchi
Department of Physics, Faculty of Science and Technology, Tokyo University of Science, Noda, Chiba 278-8510, Japan

(Received 20 February 2022; revised 22 April 2022; accepted 28 April 2022; published 10 May 2022)

The layered perovskite Sr_2RuO_4 is a very intensively studied superconductor, but its pairing mechanism, which is often coupled intimately with magnetic fluctuations in correlated materials, is still an open question. Here we present a systematic evolution of the Seebeck coefficient in Co- and Mn-substituted Sr_2RuO_4 single crystals, in which ferromagnetic and antiferromagnetic glassy states respectively emerge in proximity to the superconducting phase of the parent compound. We find that the Seebeck coefficient S divided by temperature T, S/T, shows a maximum near characteristic temperatures seen in the irreversible magnetization $M_{\rm ir}$ in both the Co- and Mn-substituted crystals, demonstrating both the ferromagnetic and antiferromagnetic fluctuations to enhance the Seebeck coefficient. Interestingly, S/T increases with lowering temperature in the parent compound, reminiscent of non-Fermi-liquid behavior, indicating an essential role of coexisting ferromagnetic and antiferromagnetic fluctuations for the itinerant electrons in Sr_2RuO_4.

DOI: 10.1103/PhysRevB.105.184507

I. INTRODUCTION

Unconventional superconductivity in the layered perovskite Sr_2RuO_4 has long attracted interest [1–6]. In particular, the recent progress from nuclear magnetic resonance (NMR) experiments has posed strong constraints on the spin sector of the superconducting order parameter [7–9], offering a clue about the consistent understanding of several experimental results [10–12] that were difficult to reconcile with earlier NMR results [13–16], as well as stimulating further symmetry-based experiments to elucidate the order parameter [17–19]. As a result, an exotic two-component order parameter with broken time reversal symmetry has been proposed, which is unique, as suggested in several studies [20,21], and various theoretical attempts have also been made [22–27], opening an avenue for exploring unconventional pairing interaction to realize such order parameters.

To address this underlying issue, it is crucially important to establish the electronic phase diagram as a function of external parameters such as pressure and chemical substitutions, as is widely discussed in correlated materials [28,29]. Indeed, although the superconducting state in Sr_2RuO_4 is extremely sensitive to impurity [30], dramatic changes in the electronic state with elemental substitutions have been reported. In isovalent systems, for instance, a spin-glass state develops over a wide range of the Ca content in $(Sr, Ca)_2RuO_4$ [31,32], which may originate from the degree of freedom in the RuO_6 octahedra. On the other hand, in $Sr_2(Ru, Ti)O_4$, an incommensurate spin-density-wave ordering due to Fermi-surface nesting appears with glassy behavior [33]. In contrast to the antiferromagnetic (AFM) coupling seen in the isovalent systems, La^{3+} substitution to Sr^{2+} sites results in electron doping to expand the electronlike γ Fermi surface, leading to ferromagnetic (FM) fluctuation owing to an enhancement of the density of states (DOS) at the Fermi energy $N(\varepsilon_{\rm F})$ near the van Hove singularity (vHs) [34–36]. These results clearly show the complicated magnetic instabilities existing in the parent compound Sr_2RuO_4, which involve complex structural and electronic origins. Such instabilities were also discussed in several studies including NMR and neutron experiments [37–41].

Among many substituted systems, Co- and Mn-substituted Sr_2RuO_4 serves as a fascinating platform to investigate how magnetic fluctuations mediate the emergence of superconductivity because slight substitutions of Co and Mn drastically transform the superconducting ground state into the FM and AFM glassy states, respectively [42]. In the Co-substituted system, the FM cluster glass characterized by an exponential relaxation of the remanent magnetization appears at low temperatures. Also, the electronic specific heat $\gamma_{\rm e}$ increases with increasing Co content, indicating an increased $N(\varepsilon_{\rm F})$ similar to La substitution [34]. It is noteworthy that the increase in $N(\varepsilon_{\rm F})$ in a 1.5% Co-substituted sample estimated from $\gamma_{\rm e}$ is comparable to that in a 5% La-substituted sample, possibly implying an effective electron-doping effect by the Co substitution [42]. Similarly, the AFM transition temperature in Mn-substituted samples is much higher than that in Ti-substituted ones, demonstrating enigmatic roles of the Co and Mn substitutions in strengthening the magnetic couplings in Sr_2RuO_4.

The aim of this study is to examine such magnetic fluctuations in $Sr_2Ru_{1-x}M_xO_4$ (M = Co, Mn) by means of the Seebeck coefficient measurement, which is known as a powerful tool for fluctuations because it is a measure of the entropy per charge carrier [43]. The observed temperature dependence of S/T (S and T are the Seebeck coefficient and temperature, respectively) has a maximum near characteristic temperatures in the magnetization in both Co- and Mn-substituted samples,

*Present address: Institute for Materials Research, Tohoku University, Sendai 980 8577, Japan; takayoshi.yamanaka.b5@tohoku.ac.jp
†okazaki@rs.tus.ac.jp

indicating that both FM and AFM fluctuations are responsible for the enhancement of the Seebeck coefficient. Moreover, in sharp contrast to the typical metallic behavior in which S/T remains constant, S/T increases with cooling in the parent compound, implying both FM and AFM fluctuations remain in the itinerant electrons in Sr_2RuO_4.

II. EXPERIMENTAL DETAILS

Single crystals of $Sr_2Ru_{1-x}M_xO_4$ (M = Co, Mn) were grown with a floating-zone method using an image furnace with a pair of halogen lamps and elliptical mirrors [42,44]. We used high-purity $SrCO_3$ (99.99%+), RuO_2 (99.9%), MnO_2 (99.99%), and CoO (99.9%) as starting materials. An excess amount of RuO_2 of 15% was weighed to compensate for the evaporation of Ru during single-crystal growth. The concentrations of Mn and Co in the obtained crystals were determined by an electron probe microanalyzer. The measured Mn concentration was 2.9%, corresponding well to the nominal concentration of 3%. In contrast, the measured Co concentrations were 1.8% and 0.8% for the nominally 3% and 1% Co-substituted samples, respectively. The relation between the nominal and measured concentrations is consistent with the trend reported in Ref. [42].

The typical dimensions of the measured crystals were $\approx 3 \times 0.2 \times 0.2$ mm^3. The Seebeck coefficient was measured by a steady-state technique using a manganin-constantan differential thermocouple in a closed-cycle refrigerator. The thermoelectric voltage of the sample was measured with Keithley 2182A nanovoltmeter. The temperature gradient (with a typical temperature gradient of 0.5 K/mm) was applied along the *ab*-plane direction using a resistive heater. The thermoelectric voltage from the wire leads was subtracted. Magnetization was measured using a superconducting quantum interference device magnetometer (Quantum Design, MPMS) under field-cooled (FC) and zero-field-cooled (ZFC) processes with an external field of $\mu_0 H = 0.1$ T applied along the c axis.

III. RESULTS AND DISCUSSION

Figure 1 summarizes the temperature variations of the Seebeck coefficient S in $Sr_2Ru_{1-x}M_xO_4$ (M = Co, Mn) single crystals. The overall behavior of S in the parent compound Sr_2RuO_4 is consistent with earlier results [45,46] and is discussed as an intriguing example to study the internal degrees of freedom in correlated metals [47]. In the substituted compounds, S increases (decreases) with Co (Mn) substitutions near room temperature, probably because of the electron (hole) doping effect as suggested in Ref. [42].

In Refs. [45,46], the Seebeck coefficient in the parent compound was analyzed in the differential form dS/dT, and an anomaly was found near 20–25 K. Xu *et al.* suggested that a band-dependent coherence develops below the anomaly temperature on the basis of the results of the Seebeck and Nernst measurements [46]. Indeed, such a coherence seems to be vital in this system [48]. To see this anomaly at 20–25 K, we compare the present data for Sr_2RuO_4 with the results extracted from Refs. [45,46] in Fig. 2(a). Although there is sample dependence in the magnitude, all the data exhibit a kink around 20–25 K, in good agreement with the present result. Also note that the effect of the impurity phase of $SrRuO_3$ is negligible because the Seebeck coefficient S in a composite sample with conductivity σ is given as $\sigma S = \sum_k \alpha_k \sigma_k S_k$ in a parallel-circuit model, where α_k, σ_k, and S_k are the volume fraction, the conductivity, and the Seebeck coefficient for the material k [49], respectively, and the volume fraction of the impurity phase in the present crystal was negligibly small.

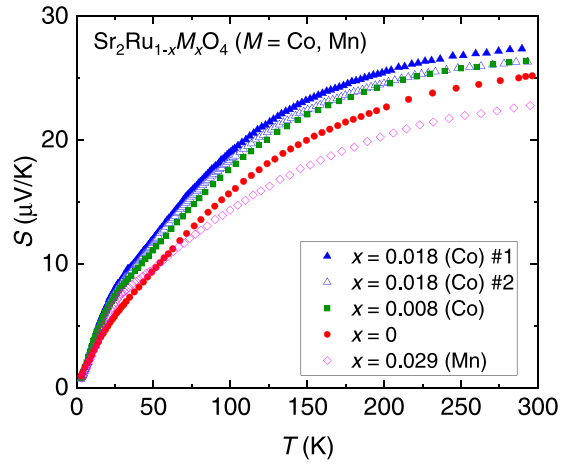

FIG. 1. Temperature dependence of the Seebeck coefficient S of $Sr_2Ru_{1-x}M_xO_4$ (M = Co, Mn) single crystals.

Here we discuss the Seebeck coefficient in the form of S/T instead of dS/dT since the Seebeck coefficient in the free-electron model (oversimplified model to multiband Sr_2RuO_4) is expressed as $S \approx -\frac{k_B^2 T}{e}\frac{N(\mu)}{n}$, where k_B, e, n, μ, and N are the Boltzmann constant, elementary charge, carrier density, chemical potential, and DOS, respectively

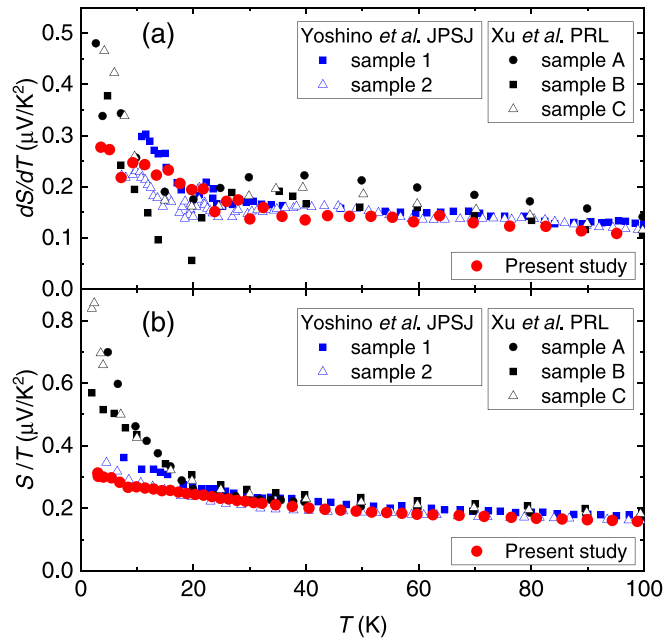

FIG. 2. Comparison of the temperature dependence of (a) dS/dT and (b) S/T of Sr_2RuO_4 single crystals. The red circles show the present data, and the other symbols are data extracted from Refs. [45,46].

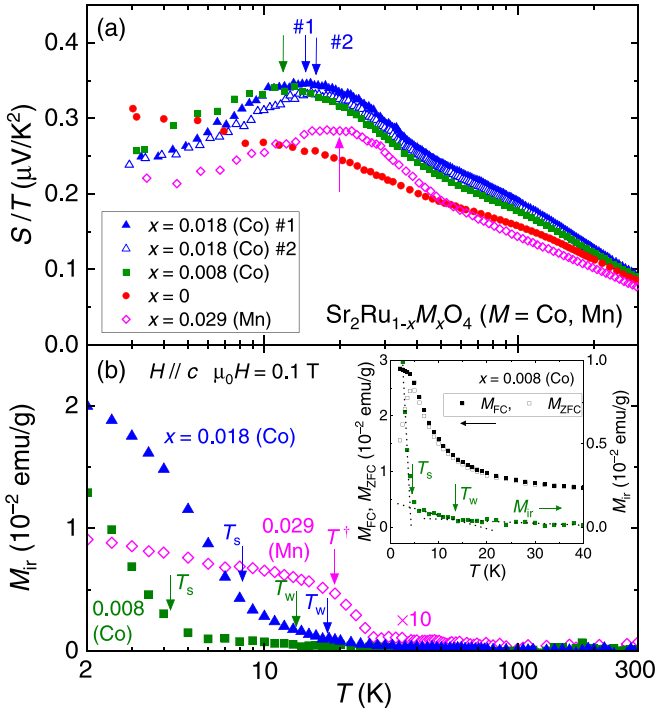

FIG. 3. (a) Temperature dependence of S/T of $Sr_2Ru_{1-x}M_xO_4$ (M = Co, Mn) single crystals. The arrows show the peak temperature T_{peak}. (b) Temperature dependence of the irreversible magnetization $M_{ir} \equiv M_{FC} - M_{ZFC}$. The arrows represent the characteristic temperatures $T^\dagger$, T_s, and T_w. (See text for details.) In the inset, M_{FC} and M_{ZFC} (left axis) and M_{ir} (right axis) of the 0.8% Co-substituted sample are shown together with the definitions of T_s and T_w.

[50]. In this form, we can follow the temperature dependence of the DOS or carrier density, which is widely analyzed in correlated electron systems, similar to the case of the pseudogap state in transition-metal oxides [51–53] and heavy-fermion formation in rare-earth compounds [54]. Note that the differential dS/dT includes the temperature derivatives of $N(\mu)$ and n in complicated forms. Figure 2(b) represents the temperature dependence of S/T in Sr_2RuO_4 in the present crystals and the calculated S/T from the extracted data from Refs. [45,46]. Interestingly, all the data are temperature dependent; in sharp contrast to conventional metals, in which S/T remains constant [43], S/T significantly increases with decreasing temperature, the origin of which will be discussed later.

We then focus on the temperature variation of S/T in the substituted systems. Figure 3(a) represents the temperature dependence of S/T in $Sr_2Ru_{1-x}M_xO_4$ (M = Co, Mn), in which we find a drastic change due to substitutions. At low temperatures, S/T exhibits a prominent peak structure in the temperature dependence for both substituted systems. The peak temperature T_{peak}, defined as the temperature at which S/T exhibits a maximum, is shown by arrows in Fig. 3(a). Note that the phonon-drag effect is unlikely to enhance the Seebeck coefficient in the substituted systems because the substitutions generally suppress the phonon mean free path [55].

To shed light on the relation to the magnetism, we plot the irreversible magnetization M_{ir}, defined as $M_{ir} \equiv M_{FC} - M_{ZFC}$, in Fig. 3(b). ($M_{FC}$ and M_{ZFC} are the magnetizations measured under FC and ZFC processes, respectively.) While the onset of the irreversibility may correspond to a transition to the FM and AFM glassy states for the Co- and Mn-substituted systems, respectively [42], a close look at the M_{ir} data reveals that the onset of the irreversibility is accompanied by a double step. The inset in Fig. 3(b) shows the temperature variations of M_{FC}, M_{ZFC}, and M_{ir} for $x = 0.008$ (Co) at low temperatures. The M_{ZFC} data decrease more steeply than those in Ref. [42], but this may be due to the low applied field in our measurement. From the plots of M_{ir} in the inset, we can see that a weak irreversibility sets in at $T_w \approx 14$ K, and subsequently, the irreversibility is strongly enhanced below $T_s \approx 4$ K. The weak and strong irreversibility temperatures T_w and T_s are defined as the points of intersection of the two linear lines as shown by the dotted line in the inset. Importantly, such coexistence of weak and strong irreversibilities is often observed in ferromagnetic spin-glass systems [56–59] and is theoretically interpreted in terms of the multicomponent vector spin model given by Gabay and Toulouse [60], in which the transverse spin components are first frozen at T_w on cooling, followed by the freezing of the longitudinal spin components at T_s, although it is still under debate whether this represents a true thermodynamic phase transition.

On the other hand, the temperature dependence of M_{ir} in the Mn-substituted sample is different from that in the Co-substituted samples: On cooling, the irreversibility sets in at $T \approx 27$ K, which is almost identical to the onset temperature T_{ir} of the static order [42], and then shows weak temperature dependence below $T^\dagger \approx 18$ K, at which M_{ir} displays a kink structure, as shown in Fig. 3(b). In the Mn-substituted sample, T_{peak} in S/T is close to this anomaly temperature $T^\dagger$, although the origin of $T^\dagger$ is unclear at present. Note that the remanent magnetization is also distinct among the Co- and Mn-substituted systems: While the temperature dependence of remanent magnetization is monotonic in the Co-substituted samples, it exhibits an anomalous peak structure below the onset temperature T_{ir} for the Mn-substituted systems [42], implying the existence of a characteristic temperature below T_{ir}. The nature of the magnetic glassy state is an issue for future study using microscopic NMR and neutron measurements.

In Fig. 4, we plot the peak temperature T_{peak} in S/T together with T_s, T_w, and $T^\dagger$ in the phase diagram reported in Ref. [42]. The peak temperature T_{peak} in S/T coincides well with the weak-irreversibility temperature T_w and the anomaly temperature $T^\dagger$ for the Co- and Mn-substituted samples, respectively, indicating an intimate relationship between the Seebeck coefficient and the magnetic fluctuations. Here since the Co and Mn substitutions induce the FM cluster glass and the spin-glass states with short-range AFM order, respectively [42], the present results indicate that both FM and AFM fluctuations are substantial for the enhancement of the Seebeck coefficient at T_{peak}. Indeed, it bears a striking resemblance to that in itinerant magnets such as the perovskite ruthenate $CaRu_{0.8}Sc_{0.2}O_3$ [61] and the doped Heusler alloy Fe_2VAl [62]; in these compounds, the Seebeck coefficient is enhanced near the ferromagnetic transition temperature through a sort of magnon-drag effect and is reduced by

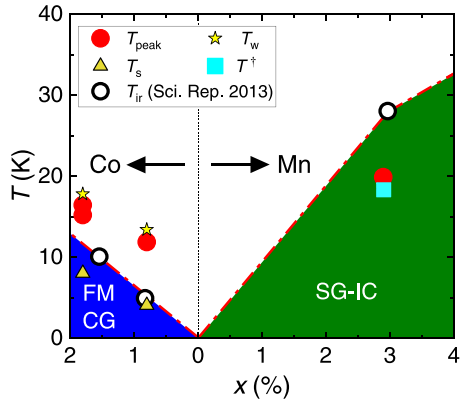

FIG. 4. Phase diagram of $Sr_2Ru_{1-x}M_xO_4$ (M = Co, Mn). The solid circles shows the peak temperature T_{peak} at which S/T exhibits maximum. The weak and strong irreversibility temperatures T_w (stars) and T_s (triangles) and the anomaly temperature $T^\dagger$ (square) are determined from the irreversibility magnetization M_{ir}. The onset temperature T_{ir} (open circles) and the regions of FM cluster glass (CG) and the spin-glass state with short-range incommensurate AFM order (SG-IC) are extracted from Ref. [42].

applying magnetic field owing to the field-induced suppression of the magnetic fluctuation. In the antiferroquadrupole (AFQ) $PrIr_2Zn_{20}$, moreover, S/T exhibits a peak structure near the AFQ transition temperature for high magnetic field, where the quadrupolar fluctuation could be enhanced [63].

Now let us recall the S/T behavior in Sr_2RuO_4 (Fig. 2), which increases with cooling down to the lowest temperature of the present measurement (∼3 K). While Seebeck coefficients are not strictly linear in temperature even in simple metals [64], the nonlinearity in Sr_2RuO_4 is unusual. As mentioned above, we show suggestive evidence that both FM and AFM fluctuations drive the enhanced Seebeck coefficient in the vicinity of the parent compound. It is therefore reasonable to consider that, even in the parent compound Sr_2RuO_4, S/T is enhanced similarly down to zero temperature, at which both FM and AFM glassy states tend to terminate for Sr_2RuO_4 [42]. Thus, this is a kind of non-Fermi-liquid (NFL) behavior close to the quantum critical point [65], which has also been observed in various correlated materials such as heavy fermions [66–70] and oxides [71]. Quite intriguingly, in contrast to the aforementioned systems, both FM and AFM fluctuations seem to be substantial for the itinerant electrons in Sr_2RuO_4, as seen in the pronounced peak of S/T observed in both Co- and Mn-substituted compounds.

One may, however, pose a simple question regarding the specific heat. In Sr_2RuO_4, the electronic specific heat shows conventional Fermi-liquid (FL) behavior [72], which is distinct from the NFL behavior observed in the Seebeck coefficient; since the Seebeck coefficient is also given as the specific heat per carrier [50], both quantities are expected to show similar anomalies [73]. On the other hand, an AFM quantum criticality may affect the ratio of these quantities at the zero-temperature limit [74]. It is interesting to note that this effect of the AFM quantum criticality may be enhanced by its multiband nature; in Sr_2RuO_4, the Fermi surfaces are composed of three cylindrical sheets: holelike α and electronlike β and γ sheets with orders of magnitude of the effective mass of $m_\alpha < m_\beta < m_\gamma$ [75–78]. Since the lighter band contributes to the transport more significantly in general [20,79], the lighter α and β bands are essential here, and importantly, these α and β sheets possess AFM instability due to nesting [38–41]. This band-dependent magnetic fluctuation may be the origin of the anomalous low-temperature increase in S/T. On the other hand, it is unclear at present how the thermoelectric transport is affected by the FM fluctuation, the importance of which is clearly demonstrated in the Co-substituted systems; the existence of the FM fluctuation is indicated by NMR [37], although neutron experiments revealed that it is very weak [38–41].

It is also known that the electrical resistivity of Sr_2RuO_4 is well described within the FL scheme [72], in which the resistivity is given as $\rho(T) = \rho_0 + AT^\nu$, with the exponent $\nu = 2$. On the other hand, the determination of ν is delicate [80], and as seen in other correlated materials, ν apparently depends on the residual resistivity even at the high-purity level [81]. It may be useful to examine the exponent in high-purity crystals [82]. We also mention that the thermal conductivity in the normal state is interesting in the sense that it also mirrors the entropy flow, while earlier studies were mainly devoted to the superconducting state [83–85]. Also, the Seebeck coefficient in the system with the Fermi level at the vHs, which is not achieved with the present Co substitution, is worth exploring because the topological change in the Fermi surface at the vHs may lead to a significant enhancement of the Seebeck coefficient [86,87]. This effect of the vHs could be investigated in electron-doped $Sr_{2-x}La_xRuO_4$.

IV. CONCLUSION

To summarize, we performed Seebeck coefficient measurements in $Sr_2Ru_{1-x}M_xO_4$ (M = Co, Mn). Although the S/T of the parent compound Sr_2RuO_4 increases with cooling down to the lowest temperature of ∼3 K as in previous reports, for Co- and Mn-substituted systems, S/T is enhanced near T_w and $T^\dagger$ in the irreversible magnetization. The emergence of the peak structure in S/T can be related to glassy FM and AFM fluctuations in the Co- and Mn-substituted systems, respectively, and therefore, the increase in S/T in Sr_2RuO_4 persisting at least down to ∼3 K suggests that both FM and AFM fluctuations are substantial in Sr_2RuO_4.

ACKNOWLEDGMENTS

The authors acknowledge Y. Maeno and K. Ishida for fruitful discussions. This work was supported by JSPS KAKENHI Grants No. JP17H06136 and No. JP18K13504.

[1] Y. Maeno, H. Hashimoto, K. Yoshida, S. Nishizaki, T. Fujita, J. G. Bednorz, and F. Lichtenberg, Superconductivity in a layered perovskite without copper, Nature (London) **372**, 532 (1994).

[2] T. M. Rice and M. Sigrist, Sr_2RuO_4: An electronic analogue of ^{3}He?, J. Phys.: Condens. Matter **7**, L643 (1995).

[3] A. P. Mackenzie and Y. Maeno, The superconductivity of Sr_2RuO_4 and the physics of spin-triplet pairing, Rev. Mod. Phys. **75**, 657 (2003).

[4] C. Kallin, Chiral p-wave order in Sr_2RuO_4, Rep. Prog. Phys. **75**, 042501 (2012).

[5] A. P. Mackenzie, T. Scaffidi, C. W. Hicks, and Y. Maeno, Even odder after twenty-three years: The superconducting order parameter puzzle of Sr_2RuO_4, npj Quantum Mater. **2**, 40 (2017).

[6] S. A. Kivelson, A. C. Yuan, B. Ramshaw, and R. Thomale, A proposal for reconciling diverse experiments on the superconducting state in Sr_2RuO_4, npj Quantum Mater. **5**, 43 (2020).

[7] A. Pustogow, Y. Luo, A. Chronister, Y.-S. Su, D. A. Sokolov, F. Jerzembeck, A. P. Mackenzie, C. W. Hicks, N. Kikugawa, S. Raghu, E. D. Bauer, and S. E. Brown, Constraints on the superconducting order parameter in Sr_2RuO_4 from oxygen-17 nuclear magnetic resonance, Nature (London) **574**, 72 (2019).

[8] K. Ishida, M. Manago, K. Kinjo, and Y. Maeno, Reduction of the ^{17}O Knight shift in the superconducting state and the heat-up effect by NMR pulses on Sr_2RuO_4, J. Phys. Soc. Jpn. **89**, 034712 (2020).

[9] A. Chronister, A. Pustogow, N. Kikugawa, D. A. Sokolov, F. Jerzembeck, C. W. Hicks, A. P. Mackenzie, E. D. Bauer, and S. E. Brown, Evidence for even parity unconventional superconductivity in Sr_2RuO_4, Proc. Natl. Acad. Sci. USA **118**, e2025313118 (2021).

[10] S. Kittaka, T. Nakamura, Y. Aono, S. Yonezawa, K. Ishida, and Y. Maeno, Angular dependence of the upper critical field of Sr_2RuO_4, Phys. Rev. B **80**, 174514 (2009).

[11] S. Yonezawa, T. Kajikawa, and Y. Maeno, First-Order Superconducting Transition of Sr_2RuO_4, Phys. Rev. Lett. **110**, 077003 (2013).

[12] C. W. Hicks, D. O. Brodsky, E. A. Yelland, A. S. Gibbs, J. A. N. Bruin, M. E. Barber, S. D. Edkins, K. Nishimura, S. Yonezawa, Y. Maeno, and A. P. Mackenzie, Strong increase of T_c of Sr_2RuO_4 under both tensile and compressive strain, Science **344**, 283 (2014).

[13] K. Ishida, H. Mukuda, Y. Kitaoka, K. Asayama, Z. Q. Mao, Y. Mori, and Y. Maeno, Spin-triplet superconductivity in Sr_2RuO_4 identified by ^{17}O Knight shift, Nature (London) **396**, 658 (1998).

[14] H. Murakawa, K. Ishida, K. Kitagawa, H. Ikeda, Z. Q. Mao, and Y. Maeno, ^{101}Ru Knight shift measurement of superconducting Sr_2RuO_4 under small magnetic fields parallel to the RuO_2 Plane, J. Phys. Soc. Jpn. **76**, 024716 (2007).

[15] K. Ishida, H. Murakawa, H. Mukuda, Y. Kitaoka, Z. Q. Mao, and Y. Maeno, NMR and NQR studies on superconducting Sr_2RuO_4, J. Phys. and Chem. Solids **69**, 3108 (2008).

[16] K. Ishida, M. Manago, T. Yamanaka, H. Fukazawa, Z. Q. Mao, Y. Maeno, and K. Miyake, Spin polarization enhanced by spin-triplet pairing in Sr_2RuO_4 probed by NMR, Phys. Rev. B **92**, 100502(R) (2015).

[17] S. Benhabib, C. Lupien, I. Paul, L. Berges, M. Dion, M. Nardone, A. Zitouni, Z. Q. Mao, Y. Maeno, A. Georges, L. Taillefer, and C. Proust, Ultrasound evidence for a two-component superconducting order parameter in Sr_2RuO_4, Nat. Phys. **17**, 194 (2021).

[18] S. Ghosh, A. Shekhter, F. Jerzembeck, N. Kikugawa, D. A. Sokolov, M. Brando, A. P. Mackenzie, C. W. Hicks, and B. J. Ramshaw, Thermodynamic evidence for a two-component superconducting order parameter in Sr_2RuO_4, Nat. Phys. **17**, 199 (2021).

[19] V. Grinenko, S. Ghosh, R. Sarkar, J.-C. Orain, A. Nikitin, M. Elender, D. Das, Z. Guguchia, F. Brückner, M. E. Barber, J. Park, N. Kikugawa, D. A. Sokolov, J. S. Bobowski, T. Miyoshi, Y. Maeno, A. P. Mackenzie, H. Luetkens, C. W. Hicks, and H.-H. Klauss, Split superconducting and time-reversal symmetry-breaking transitions in Sr_2RuO_4 under stress, Nat. Phys. **17**, 748 (2021).

[20] Y. Kasahara, T. Iwasawa, H. Shishido, T. Shibauchi, K. Behnia, Y. Haga, T. D. Matsuda, Y. Onuki, M. Sigrist, and Y. Matsuda, Exotic Superconducting Properties in the Electron-Hole-Compensated Heavy-Fermion "Semimetal" URu_2Si_2, Phys. Rev. Lett. **99**, 116402 (2007).

[21] M. Smidman, M. B. Salamon, H. Q. Yuan, and D. F. Agterberg, Superconductivity and spin-orbit coupling in non-centrosymmetric materials: A review, Rep. Prog. Phys. **80**, 036501 (2017).

[22] O. Gingras, R. Nourafkan, A.-M. S. Tremblay, and M. Côté, Superconducting Symmetries of Sr_2RuO_4 from First-Principles Electronic Structure, Phys. Rev. Lett. **123**, 217005 (2019).

[23] A. T. Rømer, D. D. Scherer, I. M. Eremin, P. J. Hirschfeld, and B. M. Andersen, Knight Shift and Leading Superconducting Instability from Spin Fluctuations in Sr_2RuO_4, Phys. Rev. Lett. **123**, 247001 (2019).

[24] H. G. Suh, H. Menke, P. M. R. Brydon, C. Timm, A. Ramires, and D. F. Agterberg, Stabilizing even-parity chiral superconductivity in Sr_2RuO_4, Phys. Rev. Research **2**, 032023(R) (2020).

[25] R. Willa, M. Hecker, R. M. Fernandes, and J. Schmalian, Inhomogeneous time-reversal symmetry breaking in Sr_2RuO_4, Phys. Rev. B **104**, 024511 (2021).

[26] A. T. Rámer, P. J. Hirschfeld, and B. M. Andersen, Superconducting state of Sr_2RuO_4 in the presence of longer-range Coulomb interactions, Phys. Rev. B **104**, 064507 (2021).

[27] S.-J. Zhang, D. Wang, and Q.-H. Wang, Possible two-component spin-singlet pairings in Sr_2RuO_4, Phys. Rev. B **104**, 094504 (2021).

[28] T. Das and C. Panagopoulos, Two types of superconducting domes in unconventional superconductors, New J. Phys. **18**, 103033 (2016).

[29] S. Paschen and Q. Si, Quantum phases driven by strong correlations, Nat. Rev. Phys. **3**, 9 (2021).

[30] A. P. Mackenzie, R. K. W. Haselwimmer, A. W. Tyler, G. G. Lonzarich, Y. Mori, S. Nishizaki, and Y. Maeno, Extremely Strong Dependence of Superconductivity on Disorder in Sr_2RuO_4, Phys. Rev. Lett. **80**, 161 (1998).

[31] S. Nakatsuji and Y. Maeno, Quasi-Two-Dimensional Mott Transition System $Sr_{2-x}Ca_xRuO_4$, Phys. Rev. Lett. **84**, 2666 (2000).

[32] J. P. Carlo, T. Goko, I. M. Gat-Malureanu, P. L. Russo, A. T. Savici, A. A. Aczel, G. J. MacDougall, J. A. Rodriguez, T. J. Williams, G. M. Luke, C. R. Wiebe, Y. Yoshida, S. Nakatsuji, Y. Maeno, T. Taniguchi, and Y. J. Uemura, New magnetic phase diagram of $(Sr, Ca)_2RuO_4$, Nat. Mater. **11**, 323 (2012).

[33] M. Minakata and Y. Maeno, Magnetic ordering in Sr_2RuO_4 induced by nonmagnetic impurities, Phys. Rev. B **63**, 180504(R) (2001).

[34] N. Kikugawa, A. P. Mackenzie, C. Bergemann, R. A. Borzi, S. A. Grigera, and Y. Maeno, Rigid-band shift of the Fermi level

in the strongly correlated metal: $Sr_{2-y}La_yRuO_4$, Phys. Rev. B **70**, 060508(R) (2004).

[35] N. Kikugawa, C. Bergemann, A. P. Mackenzie, and Y. Maeno, Band-selective modification of the magnetic fluctuations in Sr_2RuO_4: A study of substitution effects, Phys. Rev. B **70**, 134520 (2004).

[36] K. M. Shen, N. Kikugawa, C. Bergemann, L. Balicas, F. Baumberger, W. Meevasana, N. J. C. Ingle, Y. Maeno, Z.-X. Shen, and A. P. Mackenzie, Evolution of the Fermi Surface and Quasiparticle Renormalization through a Van Hove Singularity in $Sr_{2-y}La_yRuO_4$, Phys. Rev. Lett. **99**, 187001 (2007).

[37] T. Imai, A. W. Hunt, K. R. Thurber, and F. C. Chou, ^{17}O NMR Evidence for Orbital Dependent Ferromagnetic Correlations in Sr_2RuO_4, Phys. Rev. Lett. **81**, 3006 (1998).

[38] Y. Sidis, M. Braden, P. Bourges, B. Hennion, S. NishiZaki, Y. Maeno, and Y. Mori, Evidence for Incommensurate Spin Fluctuations in Sr_2RuO_4, Phys. Rev. Lett. **83**, 3320 (1999).

[39] M. Braden, Y. Sidis, P. Bourges, P. Pfeuty, J. Kulda, Z. Mao, and Y. Maeno, Inelastic neutron scattering study of magnetic excitations in Sr_2RuO_4, Phys. Rev. B **66**, 064522 (2002).

[40] P. Steffens, Y. Sidis, J. Kulda, Z. Q. Mao, Y. Maeno, I. I. Mazin, and M. Braden, Spin Fluctuations in Sr_2RuO_4 from Polarized Neutron Scattering: Implications for Superconductivity, Phys. Rev. Lett. **122**, 047004 (2019).

[41] K. Jenni, S. Kunkemöller, P. Steffens, Y. Sidis, R. Bewley, Z. Q. Mao, Y. Maeno, and M. Braden, Neutron scattering studies on spin fluctuations in Sr_2RuO_4, Phys. Rev. B **103**, 104511 (2021).

[42] J. E. Ortmann, J. Y. Liu, J. Hu, M. Zhu, J. Peng, M. Matsuda, X. Ke, and Z. Q. Mao, Competition between antiferromagnetism and ferromagnetism in Sr_2RuO_4 probed by Mn and Co doping, Sci. Rep. **3**, 2950 (2013).

[43] K. Behnia, *Fundamentals of Thermoelectricity* (Oxford University Press, Oxford, 2015).

[44] Z. Q. Mao, Y. Maeno, and H. Fukazawa, Crystal growth of Sr_2RuO_4, Mater. Res. Bull. **35**, 1813 (2000).

[45] H. Yoshino, K. Murata, N. Shirakawa, Y. Nishihara, Y. Maeno, and T. Fujita, Thermopower of a Layered Perovskite Superconductor, Sr_2RuO_4, J. Phys. Soc. Jpn. **65**, 1548 (1996).

[46] X. F. Xu, Z. A. Xu, T. J. Liu, D. Fobes, Z. Q. Mao, J. L. Luo, and Y. Liu, Band-Dependent Normal-State Coherence in Sr_2RuO_4: Evidence from Nernst Effect and Thermopower Measurements, Phys. Rev. Lett. **101**, 057002 (2008).

[47] J. Mravlje and A. Georges, Thermopower and Entropy: Lessons from Sr_2RuO_4, Phys. Rev. Lett. **117**, 036401 (2016).

[48] J. Mravlje, M. Aichhorn, T. Miyake, K. Haule, G. Kotliar, and A. Georges, Coherence-Incoherence Crossover and the Mass-Renormalization Puzzles in Sr_2RuO_4, Phys. Rev. Lett. **106**, 096401 (2011).

[49] R. Okazaki, A. Horikawa, Y. Yasui, and I. Terasaki, Photo-Seebeck effect in ZnO, J. Phys. Soc. Jpn. **81**, 114722 (2012).

[50] K. Behnia, D. Jaccard, and J. Flouquet, On the thermoelectricity of correlated electrons in the zero-temperature limit, J. Phys.: Condens. Matter **16**, 5187 (2004).

[51] I. Terasaki, Cobalt Oxides and Kondo Semiconductors: A Pseudogap System as a Thermoelectric Material, Mater. Trans. **42**, 951 (2001).

[52] Y. Ikeda, K. Saito, and R. Okazaki, Thermoelectric transport in the layered $Ca_3Co_{4-x}Rh_xO_9$ single crystals, J. Appl. Phys. **119**, 225105 (2016).

[53] C. Collignon, A. Ataei, A. Gourgout, S. Badoux, M. Lizaire, A. Legros, S. Licciardello, S. Wiedmann, J.-Q. Yan, J.-S. Zhou, Q. Ma, B. D. Gaulin, N. Doiron-Leyraud, and L. Taillefer, Thermopower across the phase diagram of the cuprate $La_{1.6-x}Nd_{0.4}Sr_xCuO_4$: Signatures of the pseudogap and charge density wave phases, Phys. Rev. B **103**, 155102 (2021).

[54] V. Zlati, B. Horvati, I. Milat, B. Coqblin, G. Czycholl, and C. Grenzebach, Thermoelectric power of cerium and ytterbium intermetallics, Phys. Rev. B **68**, 104432 (2003).

[55] K. Kurita, H. Sakabayashi, and R. Okazaki, Correlation in transport coefficients of hole-doped $CuRhO_2$ single crystals, Phys. Rev. B **99**, 115103 (2019).

[56] C. Pappa, J. Hammann, and C. Jacoboni, Spin-glass-like H-T phase diagram for the frustrated insulator $CsNiFeF_6$, J. Phys. C **17**, 1303 (1984).

[57] G. C. DeFotis, G. S. Coker, J. W. Jones, C. S. Branch, H. A. King, J. S. Bergman, S. Lee, and J. R. Goodey, Static magnetic properties and relaxation of the insulating spin glass $Co_{1-x}Mn_xCl_2{\cdot}H_2O$, Phys. Rev. B **58**, 12178 (1998).

[58] S. Dhar, O. Brandt, A. Trampert, K. J. Friedland, Y. J. Sun, and K. H. Ploog, Observation of spin-glass behavior in homogeneous (Ga, Mn)N layers grown by reactive molecular-beam epitaxy, Phys. Rev. B **67**, 165205 (2003).

[59] J. Lago, S. J. Blundell, A. Eguia, M. Jansen, and T. Rojo, Three-dimensional Heisenberg spin-glass behavior in $SrFe_{0.90}Co_{0.10}O_{3.0}$, Phys. Rev. B **86**, 064412 (2012).

[60] M. Gabay and G. Toulouse, Coexistence of Spin-Glass and Ferromagnetic Orderings, Phys. Rev. Lett. **47**, 201 (1981).

[61] T. D. Yamamoto, H. Taniguchi, Y. Yasui, S. Iguchi, T. Sasaki, and I. Terasaki, Magneto-thermopower in the weak ferromagnetic oxide $CaRu_{0.8}Sc_{0.2}O_3$: An experimental test for the Kelvin formula in a magnetic material, J. Phys. Soc. Jpn. **86**, 104707 (2017).

[62] N. Tsujii, A. Nishide, J. Hayakawa, and T. Mori, Observation of enhanced thermopower due to spin fluctuation in weak itinerant ferromagnet, Sci. Adv. **5**, eaat5935 (2019).

[63] T. Ikeura, T. Matsubara, Y. Machida, K. Izawa, N. Nagasawa, K. T. Matsumoto, T. Onimaru, and T. Takabatake, Anomalous enhancement of Seebeck coefficient in $PrIr_2Zn_20$, JPS Conf. Proc. **3**, 011091 (2014).

[64] D. K. C. Macdonald, W. B. Pearson, and I. M. Templeton, Thermo-electricity at low temperatures: VIII. Thermo-electricity of the alkali metals below 2 K, Proc. R. Soc. London, Ser. A **256**, 334 (1960).

[65] I. Paul and G. Kotliar, Thermoelectric behavior near the magnetic quantum critical point, Phys. Rev. B **64**, 184414 (2001).

[66] K. Izawa, K. Behnia, Y. Matsuda, H. Shishido, R. Settai, Y. Onuki, and J. Flouquet, Thermoelectric Response near a Quantum Critical Point: The Case of $CeCoIn_5$, Phys. Rev. Lett. **99**, 147005 (2007).

[67] S. Hartmann, N. Oeschler, C. Krellner, C. Geibel, S. Paschen, and F. Steglich, Thermopower Evidence for an Abrupt Fermi Surface Change at the Quantum Critical Point of $YbRh_2Si_2$, Phys. Rev. Lett. **104**, 096401 (2010).

[68] L. Malone, L. Howald, A. Pourret, D. Aoki, V. Taufour, G. Knebel, and J. Flouquet, Thermoelectricity of the ferromagnetic superconductor UCoGe, Phys. Rev. B **85**, 024526 (2012).

[69] H. Pfau, R. Daou, M. Brando, and F. Steglich, Thermoelectric transport across the metamagnetic transition of $CeRu_2Si_2$, Phys. Rev. B **85**, 035127 (2012).

[70] Y. Shimizu, A. Pourret, G. Knebel, A. Palacio-Morales, and D. Aoki, Non-Fermi-liquid nature and exotic thermoelectric power in the heavy-fermion superconductor UBe_{13}, Phys. Rev. B **92**, 241101(R) (2015).

[71] P. Limelette, W. Saulquin, H. Muguerra, and D. Grebille, From quantum criticality to enhanced thermopower in strongly correlated layered cobalt oxide, Phys. Rev. B **81**, 115113 (2010).

[72] Y. Maeno, K. Yoshida, H. Hashimoto, S. Nishizaki, S. Ikeda, M. Nohara, T. Fujita, A. P. Mackenzie, N. E. Hussey, J. G. Bednorz, and F. Lichtenberg, Two-dimensional fermi liquid behavior of the superconductor Sr_2RuO_4, J. Phys. Soc. Jpn. **66**, 1405 (1997).

[73] K.-S. Kim and C. Pépin, Thermopower as a signature of quantum criticality in heavy fermions, Phys. Rev. B **81**, 205108 (2010).

[74] K. Miyake and H. Kohno, Theory of quasi-universal ratio of Seebeck coefficient to specific heat in zero-temperature limit in correlated metals, J. Phys. Soc. Jpn. **74**, 254 (2005).

[75] T. Oguchi, Electronic band structure of the superconductor Sr_2RuO_4, Phys. Rev. B **51**, 1385 (1995).

[76] D. J. Singh, Relationship of Sr_2RuO_4 to the superconducting layered cuprates, Phys. Rev. B **52**, 1358 (1995).

[77] A. P. Mackenzie, S. R. Julian, A. J. Diver, G. J. McMullan, M. P. Ray, G. G. Lonzarich, Y. Maeno, S. Nishizaki, and T. Fujita, Quantum Oscillations in the Layered Perovskite Superconductor Sr_2RuO_4, Phys. Rev. Lett. **76**, 3786 (1996).

[78] S. Hill, J. S. Brooks, Z. Q. Mao, and Y. Maeno, Cyclotron resonance and effective mass renormalizations in Sr_2RuO_4, Phys. B (Amsterdam, Neth.) **280**, 283 (2000).

[79] K. Yano, T. Sakakibara, T. Tayama, M. Yokoyama, H. Amitsuka, Y. Homma, P. Miranovi, M. Ichioka, Y. Tsutsumi, and K. Machida, Field-Angle-Dependent Specific Heat Measurements and Gap Determination of a Heavy Fermion Superconductor URu_2Si_2, Phys. Rev. Lett. **100**, 017004 (2008).

[80] N. Kikugawa and Y. Maeno, Non-Fermi-Liquid Behavior in Sr_2RuO_4 with Nonmagnetic Impurities, Phys. Rev. Lett. **89**, 117001 (2002).

[81] N. Tateiwa, T. D. Matsuda, Y. Ånuki, Y. Haga, and Z. Fisk, Strong correlation between anomalous quasiparticle scattering and unconventional superconductivity in the hidden-order phase of URu_2Si_2, Phys. Rev. B **85**, 054516 (2012).

[82] J. S. Bobowski, N. Kikugawa, T. Miyoshi, H. Suwa, H.-S. Xu, S. Yonezawa, D. A. Sokolov, A. P. Mackenzie, and Y. Maeno, Improved single-crystal growth of Sr_2RuO_4, Condens. Matter **4**, 6 (2019).

[83] M. A. Tanatar, M. Suzuki, S. Nagai, Z. Q. Mao, Y. Maeno, and T. Ishiguro, Anisotropy of Magnetothermal Conductivity in Sr_2RuO_4, Phys. Rev. Lett. **86**, 2649 (2001).

[84] K. Izawa, H. Takahashi, H. Yamaguchi, Yuji Matsuda, M. Suzuki, T. Sasaki, T. Fukase, Y. Yoshida, R. Settai, and Y. Onuki, Superconducting Gap Structure of Spin-Triplet Superconductor Sr_2RuO_4 Studied by Thermal Conductivity, Phys. Rev. Lett. **86**, 2653 (2001).

[85] M. Suzuki, M. A. Tanatar, N. Kikugawa, Z. Q. Mao, Y. Maeno, and T. Ishiguro, Universal Heat Transport in Sr_2RuO_4, Phys. Rev. Lett. **88**, 227004 (2002).

[86] A. A. Varlamov, V. S. Egorov, and A. V. Pantsulaya, Kinetic properties of metals near electronic topological transitions (2 1/2-order transitions), Adv. Phys. **38**, 469 (1989).

[87] N. Ito, M. Ishii, and R. Okazaki, Enhanced Seebeck coefficient by a filling-induced Lifshitz transition in K_xRhO_2, Phys. Rev. B **99**, 041112(R) (2019).